

Mechanical and bioactivity assessment of wollastonite/PVA composite synthesized from bentonite clay

(Avaliação mecânica e de bioatividade do compósito wollastonita/PVA sintetizado a partir de argila bentonítica)

L. A. Adams^{1*}, E. R. Essien², E. E. Kaufmann³

¹University of Lagos, Department of Chemistry, Akoka, Lagos, Nigeria

²Bells University of Technology, Department of Chemical and Food Sciences, P.M.B. 1015, Ota, Ogun, Nigeria

³University of Ghana, School of Engineering Sciences, Department of Biomedical Engineering, Accra, Ghana

Abstract

Glass/polymer composites can mimic the natural structure of bone by possessing a fiber-matrix configuration which provides appropriate physical and biological properties. Wollastonite ceramics are known for their promising bioactivity and biocompatibility when applied in bone regeneration. Polyvinyl alcohol (PVA) has various attractive properties including biocompatibility and degradability which may be exploited as a polymer matrix in composites for biomedical applications. Therefore, a cost-effective method of preparing wollastonite/PVA composites is desirable by starting from bentonite clay as a silica source for the glass, instead of traditional alkoxy silanes. The composite prepared was characterized by mechanical testing, scanning electron microscopy, X-ray diffractometry and Fourier-transform infrared spectroscopy to evaluate its compressive strength, morphology, phase composition and bioactivity, respectively. Results obtained revealed for the composite a compressive strength of 0.3 MPa, the ability to induce apatite on its surface when immersed in a simulated body fluid for 7 days and desirable controlled degradation. Hence, this method can be up-scaled for preparation of wollastonite/PVA composite commercially for possible use in bone regeneration.

Keywords: wollastonite, bentonite clay, polyvinyl alcohol, bioactivity, apatite.

Resumo

Os compósitos de vidro/polímero podem imitar a estrutura natural do osso possuindo uma configuração fibra-matriz que proporciona propriedades físicas e biológicas apropriadas. As cerâmicas de wollastonita são conhecidas por suas bioatividade e biocompatibilidade promissoras quando aplicadas na regeneração óssea. O álcool polivinílico (PVA) tem várias propriedades atrativas, incluindo biocompatibilidade e degradabilidade, que podem ser exploradas como uma matriz polimérica em compósitos para aplicações biomédicas. Por conseguinte, é desejável um método de custo eficaz para a preparação de compósitos de wollastonita/PVA, partindo de argila bentonítica como fonte de sílica para o vidro, em vez de alcoxissilanos tradicionais. O compósito preparado foi caracterizado por ensaios mecânicos, microscopia eletrônica de varredura, difratometria de raios X e espectroscopia no infravermelho com transformada de Fourier para avaliar a resistência à compressão, morfologia, composição de fases e bioatividade, respectivamente. Os resultados obtidos revelaram para o compósito uma resistência à compressão de 0,3 MPa, capacidade de induzir apatita em sua superfície quando imersa em fluido corporal simulado por 7 dias e degradação controlada desejável. Portanto, este método pode ser ampliado comercialmente para a preparação de compósito de wollastonita/PVA para possível uso na regeneração óssea.


Palavras-chave: wollastonita, argila bentonítica, álcool polivinílico, bioatividade, apatita.

INTRODUCTION

Bioactive glass and ceramic materials can combine with biodegradable polymers as composites to afford a new class of materials for tissue engineering applications. This provides the advantage to harness the attributes of a glass/ceramic and a polymer material in a single matrix, which cannot be obtained from their individual components. Bioactive glasses have been extensively studied as bone graft

substitutes because of their unique property of producing a specific biological response at the material interface when implanted in the body, thus resulting in the formation of a bond between the host tissue and the material [1]. Studies have shown that degradation products from bioactive glasses influence genetic expression to control osteoblast formation, differentiation and proliferation [2]. Glasses in the binary system CaO-SiO₂, especially wollastonite (CaO·SiO₂), have been reported to exhibit excellent bioactivity and biocompatibility at a higher rate than other bioglasses and glass-ceramics [3-5]. Also, the most important clinically relevant bioactive glass-ceramic, the A/W glass-ceramic

*ladams@unilag.edu.ng

 <https://orcid.org/0000-0002-0010-5721>

[6], available commercially as Cerabone®, contains apatite $[\text{Ca}_{10}(\text{PO}_4)_6(\text{OH},\text{F}_2)]$ and wollastonite crystals in a residual CaO-SiO₂-rich glassy matrix. Bioactive glasses usually contain porous matrices that are brittle and are thus unable to withstand cyclic loads [7].

A possible strategy to solve this problem is to develop a biodegradable polymer to serve as a matrix into which bioactive glass particulates are added as the filler phase [8]. Polymers possess higher plasticity, formability and toughness. On the other hand, the glass or glass-ceramic phase adds stiffness and adequate mechanical strength to the composite. Hence the polymer/bioceramic composite represents a scaffold tailored for adequate mechanical and structural behavior, degradation kinetics and bioactivity [9]. Furthermore, when glass with nanometer dimension, serving as the inorganic phase, is incorporated into a compliant polymer matrix, it mimics the structural organization of natural bone, where the inorganic component (hydroxycarbonate apatite, HCA) and its organic component (collagen) interact at a molecular scale thereby giving rise to structures that are linked by primary chemical bonds [10]. Studies have also shown that nanocomposites in which nanoparticles are dispersed in a polymer matrix can result in improved interaction with host tissue and cells [11-13].

Polyvinyl alcohol (PVA) has enjoyed a wide range of biomedical applications for reasons spanning solubility, thermo-stability, chemical resistance, film-forming ability, compatibility and degradability [14]. It is envisaged that, based on these biologically friendly properties, combining wollastonite and PVA in a composite would ultimately lead to desirable material properties and performance in biomedical applications. Clay minerals contain fine grains and sometimes nanometer size hydrous silicates in an octahedral or tetrahedral layered arrangement. Bentonite clay, in particular $(\text{Na,Ca})(\text{Al,Mg})_2(\text{Si}_4\text{O}_{10})_3(\text{OH})_6 \cdot n\text{H}_2\text{O}$, is a naturally occurring sedimentary clay with the 3-layered clay structure formed from the weathering of volcanic ash. Recently, bentonite has been shown to be a promising source of silica in bioactive glass production [15]. In that report, the glass formed exhibited textural parameters containing sub-micron sized particles and large surface area desirable for *in vivo* biological applications. Previous studies have reported the formation of glass/PVA composites from tetraethylorthosilicate (TEOS) as the SiO₂ precursor [16-22]. The current work, therefore, reports a paradigm shift from TEOS to bentonite clay as an economic source of silica. Consequently, we prepared wollastonite/PVA composite from bentonite clay and studied its bioactivity in simulated body fluid (SBF).

MATERIALS AND METHODS

Materials: bentonite clay was obtained locally from Nigeria, calcium nitrate tetrahydrate $\text{Ca}(\text{NO}_3)_2 \cdot 4\text{H}_2\text{O}$ was obtained from Loba Chemie, while sodium hydroxide (NaOH), ethanol (C₂H₅OH), and polyvinyl alcohol (PVA) with average molecular weight 125000 g.mol⁻¹ and 98%

degree of hydrolysis were all obtained from Sigma-Aldrich.

Preparation of gel: SiO₂ was extracted from the bentonite clay to form Na₂SiO₃ by boiling with 1 M NaOH (270 mL) at 120 °C for 4 h. After allowing to cool, the mixture was filtered by suction. Then $\text{Ca}(\text{NO}_3)_2 \cdot 4\text{H}_2\text{O}$ was added slowly to the filtrate over 45 min under constant stirring with a magnetic stirrer. After complete addition, the gel formed was stirred for 2 h. Afterward, it was washed in deionized water (4 x 300 mL) to remove NaNO₃ reaction by-product, as shown in Eq. A, then dried at 60 °C for 24 h.



Formation of wollastonite (BGC): wollastonite phase was obtained by treating the dry gel in a furnace, operating at a heating/cooling rate of 5 °C/min, at 700 °C for 2 h. The monolith formed thereof was milled in 100% ethanol in a mortar using a pestle for 2 h to form a slurry. Thereafter, the ethanol was allowed to evaporate under ambient conditions to leave behind fine glass powders. **Preparation of PVA solution:** aqueous PVA solution having a concentration of 7 wt% was prepared by dissolving the PVA granules in deionized water at 80 °C with continuous stirring for 2 h. **Preparation of wollastonite/PVA composite (BGC/PVA):** the composite containing 20 wt% wollastonite and 80 wt% PVA solution was prepared by initially sonicating the wollastonite powders in the PVA in an ultrasonic cleaner (ROHS, UD100SH-3LQ) at 60 °C for 5 min to form a homogeneous solution. After this, the resulting mixture was cast into cylindrical plastic molds and dried at 45 °C for 5 days.

Characterization: the samples in quintuplicates with cylindrical dimensions measuring 11x14 mm (diameter x height) were subjected to compression testing using a universal mechanical tester (Mark-10, ESM301L, USA). The load was applied at a cross-head speed of 25 mm/min until failure. The compressive strength (σ_c) was calculated from the relation:

$$\sigma_c = F/\pi r^2 \quad (\text{B})$$

where F is the applied load at failure and r is the sample radius. The elastic modulus was calculated as the slope of the initial linear section of the stress-strain curve. The microstructure of the samples was assessed in a scanning electron microscope (SEM, Jeol, JSM 6390LV, Japan) at an accelerating voltage of 15 kV. The diffraction patterns of the samples were obtained at a step size of 0.10° and a scan rate of 1 s/step with a CuK α radiation operating source of wavelength $\lambda=0.154060$ nm at 45 kV, 40 mA in the 2 θ range from 5° to 90° using an X-ray diffractometer (PANalytical, Empryrean Series 2). The strongest diffraction peak (2 θ ~29.36°) was used to calculate the crystallite size (ζ) of the main phase in the crystalline sample (wollastonite - CaSiO₃) according to the Scherrer equation:

$$\zeta = (k \cdot \lambda) / (\beta \cdot \cos\theta) \quad (\text{C})$$

where k is the Scherrer constant, equal to 0.89, λ the wavelength of the $\text{CuK}\alpha$ X-ray, and β the full width at half maximum (FWHM) of the strongest diffraction peak. Assessment of the nature of bonds present in the glass and composite networks was performed using Fourier-transform infrared spectroscopy (FTIR) with attenuated total reflectance (Bruker-Alpha, Platinum ATR) operating in the wavenumber range of 4000 to 500 cm^{-1} .

In vitro bioactivity determination in simulated body fluid (SBF): bioactivity test to confirm apatite formation on the BGC/PVA composite material was performed by soaking the sample in SBF (pH 7.4) at 36.5 °C prepared according to the standard *in vitro* procedure [23] using the following analytical grade reagents: NaCl, NaHCO_3 , KCl, $\text{K}_2\text{HPO}_4 \cdot 3\text{H}_2\text{O}$, $\text{MgCl}_2 \cdot 6\text{H}_2\text{O}$, CaCl_2 , tris-hydroxymethyl aminomethane [tris-buffer, $(\text{CH}_2\text{OH})_3\text{CNH}_2$], and 1 M HCl to obtain a similar ionic concentration as found in human blood plasma [24]. The samples, in triplicates, were immersed in SBF in a clean sterilized plastic bottle at a concentration of 0.0022 g/mL and a surface area/volume of 15.5, being porous [23], and placed in an incubator for a maximum of 7 days. The SBF solutions were monitored daily for 7 days to assess pH changes, an indicator for the reactivity of the samples. After removal from the SBF, the samples were rinsed with deionized water, then 100% ethanol and left to dry at ambient temperature for 1 day.

RESULTS AND DISCUSSION

Mechanical properties: a typical stress-strain curve for BGC/PVA is shown in Fig. 1. The curve was defined by three regimes, comprising a linear elastic stage, which corresponded to cell edge bending or face stretching. This was followed by a stress plateau, corresponding to progressive cell collapse, and finally, densification, corresponding to the collapse of the cells throughout the material [19]. The

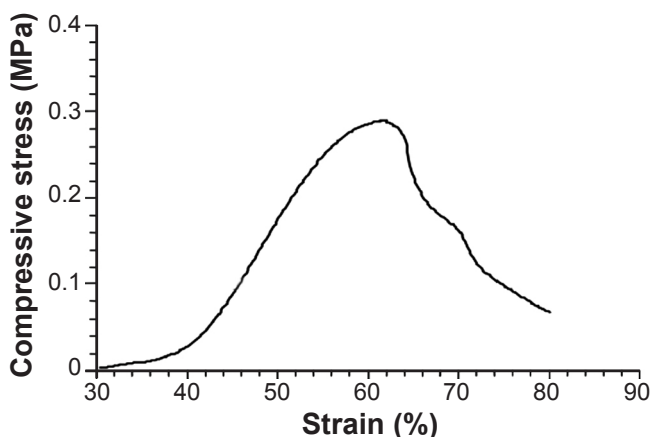


Figure 1: Representative stress-strain curve of the BGC/PVA composite. The compressive strength was 0.3 MPa, while the elastic modulus was determined to be 1.34 MPa.

[Figura 1: Curva tensão-deformação representativa do compósito BGC/PVA. A resistência à compressão foi de 0,3 MPa, enquanto o módulo de elasticidade foi determinado como sendo 1,34 MPa.]

compressive strength of the composite was 0.3 MPa with an elastic modulus of 1.34 MPa. This compressive strength value was within the region of spongy bone without the strut, known to be in the range 0.2-4 MPa. Importantly, it should be mentioned that the sintering temperature of the glass phase was set low at 700 °C for 2 h to prevent full crystallization, which could negatively affect the bioactivity of the composite. In the design of biomaterials for *in vitro* application, in addition to the mechanical property requisite, the twin properties of bioactivity and biodegradability are of utmost considerations in order to ensure appropriate performance. Interestingly, from the result obtained, the composite material had properties similar to trabecular bone and may be considered for repair and replacement of spongy bone.

Morphology: the morphology of the samples is shown in Fig. 2. The reaction of Na_2SiO_3 with $\text{Ca}(\text{NO}_3)_2 \cdot 4\text{H}_2\text{O}$ led to the formation of CaSiO_3 gel (Eq. A), which on heat treatment at 700 °C resulted in crystallization to give wollastonite ($\text{CaO} \cdot \text{SiO}_2$ - BGC). BGC exhibited a fracture face as observed in Fig. 2a. This phenomenon is usually caused by particle deformation during the heat treatment process that sets during densification, which occurs by a viscous flow sintering mechanism in the glass. In this case, the viscous flow was low due to the low sintering temperature of 700 °C for 2 h set for BGC. A significant change in surface morphology was evident after adding PVA (Fig. 2b). As observed, the surface became thicker and rough with few agglomerates, but still showing well-distributed grains due to the ability of the PVA to coalesce the glass particles into the polymer matrix, thus resulting in a higher surface area-to-volume ratio than BGC. The improvement in morphology after introducing PVA can better be appreciated from a comparison of the three-dimensional plots of the surface of BGC and BGC/PVA depicted in Figs. 2d and 2e, respectively. The morphology exhibited by BGC/PVA could be useful for improved mechanical performance, accelerated rate of bioactivity in biological fluids and enhanced cell and protein attachment or adsorption if the material is used as a temporary graft to promote bone repair [24]. The microstructural transition of BGC/PVA following immersion in SBF for 7 days is shown in Fig. 2c. Apatite particles, highly agglomerated, with the hexagonal plate-like crystal structure, were seen on the surface of the material. Apatite formation on the surface of a material, when immersed in physiological fluids, is regarded as evidence of bioactivity [24]. Hence the composite herein should be capable of initiating bone bonding reactions when applied as a scaffold to restore a defective bone.

Diffraction patterns: the X-ray diffraction (XRD) patterns of the samples are presented in Fig. 3. The diffraction pattern of BGC (Fig. 3a) matched the standard PDF (JCPDS #00-043-1460) when indexed in angular location and intensity, indicating the presence of a single wollastonite crystalline phase [25] at the 2θ angles with the corresponding reflection indices in the hkl planes: 11.53° (200), 23.08° (400), 26.45° (-202), 29.79° (320),

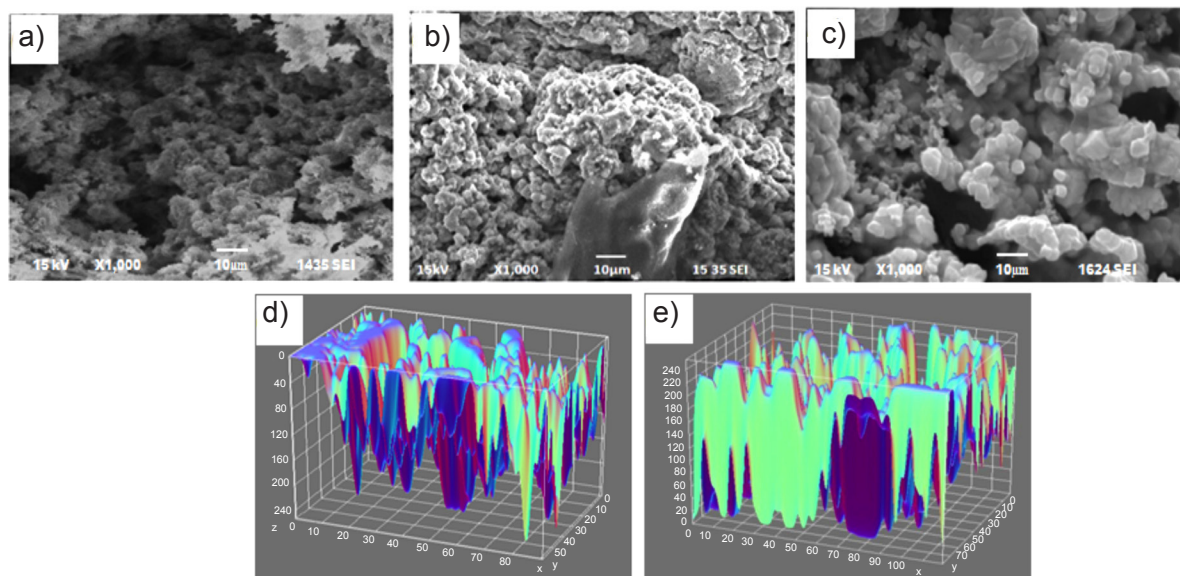


Figure 2: SEM micrographs of BGC (a), BGC/PVA composite (b), and BGC/PVA composite showing the growth of apatite after immersion for 7 days in SBF (c); and 3D surface plots of BGC (d), and BGC/PVA (e).

[Figura 2: Micrografias de MEV de BGC (a), compósito BGC/PVA (b) e compósito BGC/PVA mostrando o crescimento de apatita após imersão durante 7 dias em SBF (c); e gráficos de superfície 3D de BGC (d) e BGC/PVA (e).]

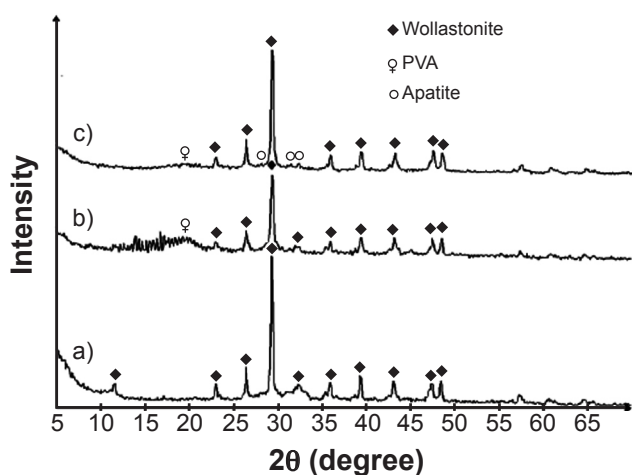


Figure 3: XRD patterns of BGC after sintering at 700 °C (a), and BGC/PVA composite before (b) and after (c) immersion in SBF for 7 days showing the phases present.

[Figura 3: Padrões de DRX de BGC após sinterização a 700 °C (a), e compósito BGC/PVA antes (b) e após (c) imersão em SBF durante 7 dias mostrando as fases presentes.]

32.42° (-402), 36.10° (402), 39.41° (-520), 47.51° (800), and 48.46° (720). Judging from the nature of the peaks, the glassy phase exhibited low crystallinity. After addition of PVA, the intensity of the wollastonite peaks decreased slightly (Fig. 3b), while the PVA component was detected as a weak and broad peak around 2θ 15°-20°, centered at 19.52° (101) [26], which indicated poor crystalline behavior. After incubation in SBF for 7 days, apatite peaks emerged at 2θ 28.22° (102), 31.54° (121), and 62° (300), Fig. 3c. The configuration of the apatite peaks matched the standard PDF (JCPDS #9-0432) in angular location, intensity and reflection indices (hkl), and hence support the formation

of apatite as indicated earlier in the SEM result in Fig. 2c. Furthermore, the PVA peak at 2θ 19.52° became diffuse after soaking BGC/PVA for 7 days in SBF (Fig. 3c). This outcome was remarkable because it showed the ability of the polymer in the composite to degrade in a physiological fluid, which is a crucial requirement for a material intended to serve as a temporary graft in bone repair [2]. The crystallite sizes of BGC and BGC/PVA, based on the Scherrer equation (Eq. C), were 24.6 and 31.4 nm, respectively. This result supported the SEM results of Figs. 2a and 2b which showed a thicker surface layer with some agglomerates in BGC/PVA when compared with BGC.

Assessment of bonds: the FTIR spectra of BGC, PVA and BGC/PVA before and after immersion in SBF for 7 days are depicted in Fig. 4. The spectrum of BGC showed a small broad band centered at 3360 cm^{-1} considered to be OH asymmetric stretching vibration of adsorbed surface water in the sample [27]. This was further confirmed by the small shoulder around 1670 cm^{-1} , resulting from OH bending mode of water molecules. The strong peak near 1407 cm^{-1} was assigned to the carbonate group (CO_3^{2-}) which was formed from adsorption of atmospheric CO_2 during the process of extracting SiO_2 from bentonite clay by NaOH solution [28]. This was supported by a C-O deformation mode, which appeared as a sharp peak near 873 cm^{-1} . The presence of silica in the compound was confirmed at 971 and 712 cm^{-1} which are the asymmetric and symmetric stretching vibrations of Si-O-Si bonds, respectively, both having low intensity, thus confirming the low crystalline nature of the glass phase as suggested earlier in the XRD result (Fig. 3a). In the spectrum of the pure PVA, the broad band centered at 3313 cm^{-1} was associated with free OH group and bonded OH stretching vibration. The band at 2940 cm^{-1} was

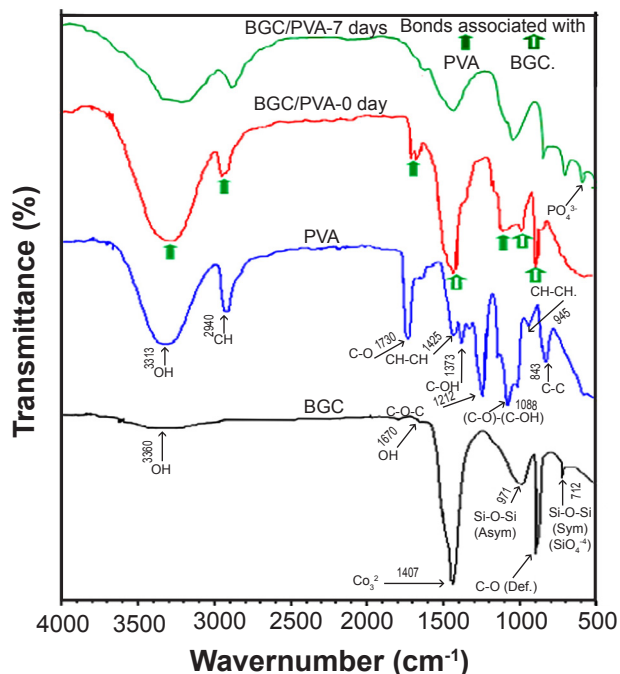


Figure 4: FTIR spectra of BGC, pure PVA, and BGC/PVA composite before and after immersion in SBF for 7 days showing the type of bonds present.

[Figura 4: Espectro de FTIR de BGC, PVA puro e compósito BGC/PVA antes e depois da imersão em SBF durante 7 dias mostrando o tipo de ligações presentes.]

ascribed to C-H asymmetric stretching in CH_2 groups. The bands at 1730 and 1088 cm^{-1} were associated with C=O and C-O stretching vibrations in incompletely hydrolyzed PVA [29]. The band at 843 cm^{-1} was assigned to C-C stretching mode. In the spectrum of the composite (BGC/PVA), bands associated with both the glass phase (BGC) and the pure PVA were observed, but the intensity of the peaks associated with BGC and PVA reduced slightly. After immersion in SBF for 7 days, the intensity of the peaks decreased significantly, signaling degradability of the composite as was observed in the XRD result in Fig. 3c. Additionally, a new peak characteristic of the vibrational mode of phosphate in hydroxyapatite emerged at 603 cm^{-1} [1, 3, 4, 10], which confirmed the formation of apatite on the glass surface, as observed previously using SEM and XRD. Apatite formation on the surface of a material is regarded as crucial for further cellular reactions to occur that ultimately lead to the formation of a tenacious bond between the implant material and the host bone [24, 30].

Reactivity of the composite in SBF: the reactivity of BGC/PVA composite monitored by pH changes for the period of immersion in SBF is shown in Fig. 5. There was a steep increase in pH for the first 2 days from 7.4 to 7.9, which was due to the material exchanging Ca^{2+} ions rapidly with H^+ or H_3O^+ ions in the SBF. As the immersion period increased up to 4 days, the increase in pH slowed slightly, reaching a saturated value of 8.1. Between 4 and 5 days, the pH stabilized at 8.1, then decreased to 7.9 on the 7th

day. The mechanism of release of Ca^{2+} ions, which resulted in pH increment is in line with that reported in a previous study [31] on the formation of an apatite-like layer on materials containing SiO_2 and CaO . Thus, as hydroxycarbonated (HCA) layer was continually crystallized from the amorphous $\text{CaO-P}_2\text{O}_5$ film deposited on the surface, and the free surface available on the material for further leaching of Ca^{2+} ions reduced. This led to a slower increase in the pH of the fluid as observed in Fig. 5. The decrease in the pH value from the 5th to 7th day was caused by re-adsorption of Ca^{2+} ions and withdrawal of P from the SBF onto the glass surface to form more apatite layers, and could also be the result of contribution from acidic degradation products of the PVA, being incompletely hydrolyzed [32, 33].

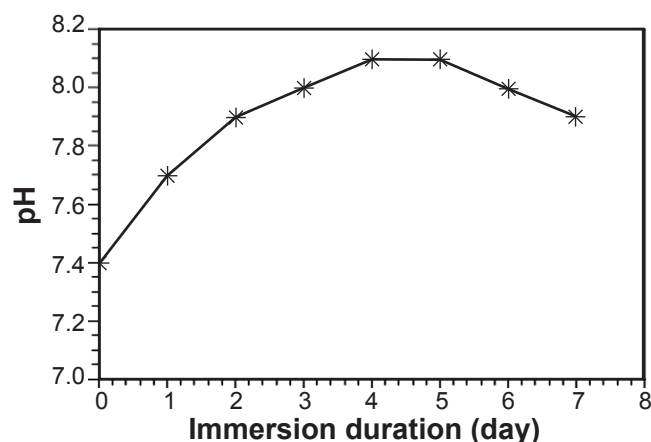


Figure 5: pH changes of BGC/PVA during the period of immersion in SBF.

[Figura 5: Alterações de pH do BGC/PVA durante o período de imersão em SBF.]

CONCLUSIONS

A bioactive wollastonite/polyvinyl alcohol ($\text{CaO.SiO}_2/\text{PVA}$) composite was prepared from bentonite clay, which served as a source of silica. The aim was, for the first time, to investigate the formation and performance of wollastonite/polymer composite in which the wollastonite was formed from silica extracted from bentonite clay as an inexpensive silica precursor. Results obtained indicated that the wollastonite was successfully incorporated as a filler phase into a PVA matrix. The compressive strength of the composite was 0.3 MPa , which is in the strength region of the trabecular bone. Immersion experiment of the composite in SBF for 7 days showed the ability to induce apatite nucleation and growth on its surface. In addition, the material exhibited controlled degradability in SBF. These properties are among the basic requirements for a material to serve as an ideal scaffold in bone repair. Hence our synthetic route could be optimized for large scale production of wollastonite/PVA composite instead of using expensive alkoxy silanes as the traditional silica precursors.

ACKNOWLEDGEMENT

We are grateful to the Department of Biomedical Engineering of the University of Ghana, Legon, for providing the facilities for this work.

REFERENCES

- [1] D. Lukito, J.M. Xue, J. Wang, *Mater. Lett.* **59** (2005) 3267.
- [2] I.D. Xynos, A.J. Edgar, L.D.K. Buttery, L.L. Hench, J.M. Polak, *J. Biomed. Mater. Res.* **55** (2001) 151.
- [3] P. Saravanapavan, L.L. Hench, *J. Biomed. Mater. Res.* **54** (2001) 608.
- [4] P.N. De Aza, F. Guitian, S. De Aza, *Scr. Metall. Mater.* **31** (1994) 1001.
- [5] P.N. De Aza, Z. Luklinska, M.R. Anseau, F. Guitian, S. De Aza, *J. Microsc.* **182** (1996) 24.
- [6] T. Nakamura, T. Yamamuro, S. Higashi, T. Kokubo, S. Itoo, *J. Biomed. Mater. Res.* **19** (1985) 685.
- [7] J.R. Jones, *Acta Biomater.* **9** (2013) 4457.
- [8] M. Navarro, C. Aparicio, M. Charles-Harris, M.P. Ginebra, E. Engel, J.A. Planell, in “Ordered polymeric nanostructures at surfaces”, G.J. Vancso (Ed.), Springer-Verlag, Berlin (2006) 209.
- [9] Z.H. Huang, K.Y. Qiu, *Polymer* **38** (1997) 521.
- [10] S.K. Misra, T. Ansari, D. Mohn, S.P. Valappil, T.J. Brunner, W.J. Stark, I. Roy, J.C. Knowles, P.D. Sibbons, E.V. Jones, A.R. Boccaccini, V. Salih, *J. R. Soc. Interface* **44** (2010) 453.
- [11] G.E. Fantner, O. Rabinovich, G. Schitter, P. Thurner, J.H. Kindt, M.M. Finch, J.C. Weaver, L.S. Golde, D.E. Morse, E.A. Lipman, I.W. Rangelow, P.K. Hansma, *Compos. Sci. Technol.* **66** (2006) 1205.
- [12] G.K. Hunter, H.A. Goldberg, *Biochem. J.* **302** (1994) 175.
- [13] B. Marelli, C.E. Ghezzi, D. Mohn, W.J. Stark, J.E. Barralet, A.R. Boccaccini, S.N. Nazhat, *Biomaterials* **32** (2011) 8915.
- [14] O.W. Guirguis, M.T.H. Moseley, *Nat. Sci.* **4** (2012) 57.
- [15] L.A. Adams, E.R. Essien, *J. Adv. Ceram.* **5** (2016) 47.
- [16] D.P. Goy, E. Gorosito, H.S. Costa, P. Mortarino, N.A. Pedemonte, J. Toledo, H.S. Mansur, M.M. Pereira, R. Battaglini, S. Feldman, *Open Biomed. Eng. J.* **6** (2012) 85.
- [17] Q. Jie, K. Lin, J. Zhong, Y. Shi, Q. Li, J. Chang, R. Wang, *J. Sol-Gel Sci. Technol.* **30** (2004) 49.
- [18] H.S. Mansur, H.S. Costa, *Chem. Eng. J.* **137** (2008) 72.
- [19] A.A.R. de Oliveira, V.S. Gomide, M.F. Leite, H.S. Mansur, M.M. Pereira, *Mater. Res.* **12** (2009) 239.
- [20] L.S. Luisa, I. Dias, H.S. Mansur, C.L. Donnici, M.M. Pereira, *Biomater* **1** (2011) 114.
- [21] M.M. Pereira J.R. Jones, R.L. Orefice, L.L. Hench, *J. Mater. Sci. Mater. Med.* **16** (2005) 1045.
- [22] A.P.V. Pereira, W.L. Vasconcelos, R.L. Oréfice, *J. Non-Cryst. Solids* **27** (2000) 180.
- [23] T. Kokubo, H. Takadama, *Biomaterials* **27** (2006) 2907.
- [24] L.L. Hench, M. Polak, *Science* **295** (2002) 1014.
- [25] B. Downs, R. Swaminathan, K. Bartelmehs, *Am. Mineral.* **78** (1993) 1104.
- [26] Y.M. Lee, S.H. Kim, S.J. Kim, *Polymer* **26** (1996) 5897.
- [27] G.D. Venkatasubbu, S. Ramasamy, V. Ramakrishnan, J. Kumar, *Biotech* **1** (2011) 173.
- [28] M. Cerruti, C. Morterra, *Langmuir* **20** (2004) 6382.
- [29] W.A. Jabbar, N.F. Habubi, S.S. Chiad, *J. Ark. Acad. Sci.* **64** (2010) 101.
- [30] L.L. Hench, *J. Am. Ceram. Soc.* **81** (1998) 1705.
- [31] C. Ohtsuki, T. Kokubo, T. Yamamuro, *J. Non-Cryst. Solids* **143** (1992) 84.
- [32] C. David, C. De Kesel, F. Lefebvre, M. Weiland, *Angew. Makromol. Chem.* **216** (1994) 21.
- [33] J. Pajak, M. Ziemiński, B. Nowak, *Chemik* **64** (2010) 523.
- (*Rec.* 27/08/2018, *Rev.* 14/10/2018, 22/11/2018, *Ac.* 07/01/2019)